Surface-site determination using electron-energy-loss spectroscopy and lattice-dynamical models

R. L. Strong, B. Firey, F. W. de Wette, and J. L. Erskine
Department of Physics, University of Texas at Austin, Austin, Texas 78712
(Received 21 May 1982)

We show that a lattice-dynamical model based on pair interactions is able to account for the central features of high-resolution electron-energy-loss spectra for oxygen adsorption on Al(111). This particular metal-adsorbate system is complicated by the simultaneous formation of an oxygen overlayer and underlayer. Of seven possible overlayer-underlayer configurations which yield (1×1) two-dimensional order, only one configuration accurately accounts for the experimental results when reasonable model parameters are assumed.

Adsorption of oxygen on Al(111) provides a good illustration of the application of several structural probes to the same system. The O/Al(111) system has been studied by low-energy electron diffraction (LEED)[1] and surface extended x-ray absorption fine structure (SEXAFS),[2] and by a number of other techniques including Auger spectroscopy,[1,3] photoemission,[2,4,5] and work function measurements.[3,6] More recently, high-resolution electron-energy-loss spectroscopy (EELS) has also been used to investigate oxygen adsorption on Al(111).[7] Two of the most interesting results of this EELS study are (1) both surface and subsurface oxygen species are present, even for very low oxygen doses with the sample at room temperature, and (2) the surface oxygen phase tends to convert to subsurface oxygen rather quickly at room temperature. Photoemission[5] and work function studies[6] also suggest a similar surface layer instability. This result probably accounts for the difficulty in obtaining a consistent structural model for chemisorbed (1×1) oxygen on Al(111).

EELS spectra for (1×1)-O/Al(111) are shown in Fig. 1. The two primary peaks at 80 and 105 meV are due to surface and subsurface oxygen, respectively. The data clearly show that both surface and subsurface oxygen phases occur between 2- and 200-L exposures (1 L = 10^{-6} Torr sec), and that higher doses or annealing increase the ratio of subsurface to surface oxygen. A closer inspection reveals two additional interesting features which were not discussed in our previous paper. First, the loss peaks are considerably broader than the elastic peak. This is generally not the case for adsorbed species on metal surfaces. Infrared studies show that loss peak widths are typically 1 meV or less, therefore loss peak widths should be the same as the elastic peak width (i.e., the spectrometer resolution). Second, in addition to the two major loss peaks, a third weaker peak is observed which shifts from ~ 40 to ~ 50 meV as the subsurface peak grows. This relationship of the low-energy peak to the subsurface peak suggests that it also is associated primarily with the subsurface phase.

In an attempt to understand these EELS spectra in more detail and to determine the relevance of the data to various structural models for the (1×1)-O/Al(111) system based on LEED and SEXAFS, we have carried out a number of lattice-dynamical model calculations. The Al substrate is modeled as a 13-

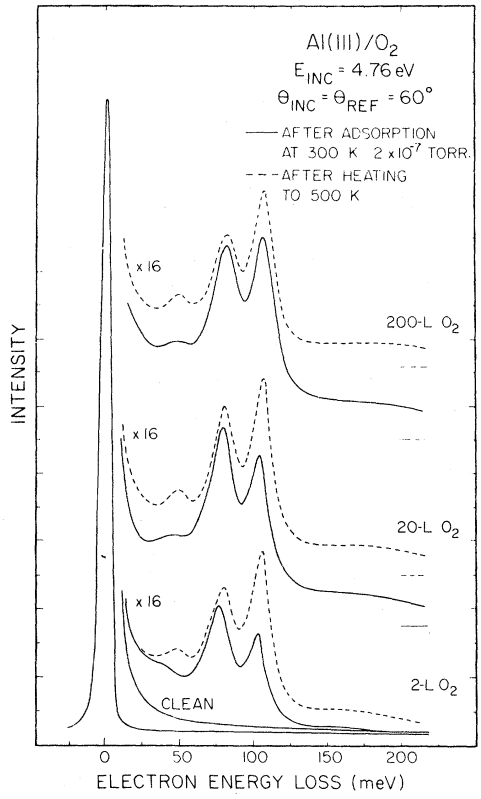

FIG. 1. EELS spectra for 2, 20, and 200 L (1 L = 10^{-6} Torr sec) O_2 on Al(111) before and after annealing. The 80-meV peak corresponds to surface oxygen; the 105-meV peak corresponds to subsurface oxygen; and the 40-meV peak results from coupling of first and second Al layers through subsurface oxygen.

layer face-centered-cubic slab with (111) orientation of the surface planes.[8] All force constants in the model are derivable from central pair potentials, and only nearest-neighbor bond stretching force constants were retained for the O-Al and O-O interactions. Pair interactions involving oxygen are associated with essentially covalent bonds and tend to be much stronger than those for Al-Al interactions. Consequently, it did not seem necessary to reproduce the behavior of the aluminum substrate with great precision, so all Al-Al interactions were taken for convenience to be of Lennard-Jones form retaining contributions up to seventh neighbors.

Vibrational frequencies and associated eigenvectors of the slab model were calculated at $\bar{\Gamma}$, the origin of the surface Brillouin zone; this corresponds to $\Delta k_{\parallel}=0$, the condition associated with specular EELS scattering geometry used in the experiments. In specular scattering only modes associated with dynamic dipole moments perpendicular to the surface ($\hat{z}$ direction in our geometry) produce loss features. Therefore, in comparing calculated frequencies to experiment, only frequencies associated with $\hat{z}$-polarized motions are considered.

Oxygen adsorbed on Al(111) yields a (1×1) LEED[1] structure, and SEXAFS[2] and EELS[7] results indicate that both underlayer and overlayer sites can be occupied by oxygen. Therefore our lattice models were based on (1×1) configurations of overlayer and underlayer oxygen. Figure 2 illustrates the Al(111) surface, and labels various high-symmetry locations for oxygen atoms above and below the surface. Above the surface, there are two inequivalent threefold sites labeled *B* and *C*. *B* sites are above a second layer Al atom and *C* sites are above a void. Below the surface, there are two inequivalent tetrahedral sites labeled t*A* and t*B*; t*A* sites are $3d/4$ below a surface Al atom and t*B* sites are $3d/4$ above a second layer Al atom [$d=2.3383$ Å is the Al(111) interplanar spacing]. Also below the surface are octahedral sites, labeled o*C*, centered between first- and second-layer threefold hollow sites. We computed frequencies and associated eigenvectors for the two overlayer configurations, the three underlayer configurations, and the six overlayer-underlayer configurations, assuming all planar sites were occupied and no host-lattice relaxation or reconstruction. We also considered the configurations consisting of *C* sites and modified octahedral sites (mo*C*) favored by self-consistent thin-film electronic structure calculations,[9] and mo*C* sites alone.

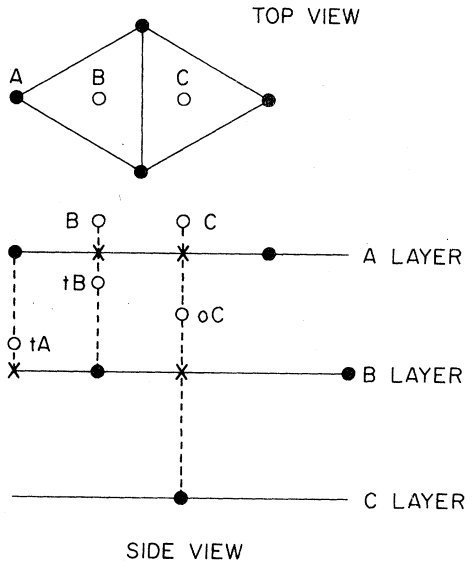

FIG. 2. Lattice model for the fcc Al(111) surface showing the five high-symmetry sites *B*, *C*, t*A*, t*B*, and o*C* (see text) which are candidates for (1×1) overlayer (*B* and *C*) and underlayer (t*A*, t*B*, and o*C*) oxygen atoms.

The lattice-dynamical model yields a single $\hat{z}$-polarized mode for both overlayer sites, two $\hat{z}$-polarized modes for the four underlayer sites, and three $\hat{z}$-polarized modes for the seven overlayer-underlayer configurations. Our approach was to fit the three loss peak frequencies in Fig. 1 by varying the O-Al and O-O force constants for the seven overlayer-underlayer configurations. It was not possible to simultaneously match the 80- and 105-meV peaks in Fig. 1 for the two overlayer-underlayer configurations with an underlayer oxygen in the t*A* site of Fig. 2. This site is intuitively the least likely high-symmetry site for an underlayer oxygen atom, since it is not directly accessible from the surface. It is not difficult to fit the computed peak energies to the 80- and 105-meV peaks for the other five configurations. However, fitting the low-energy peak to the data depends rather critically on the strength of the O-O force constant.

One would expect the O-O force constant to be greatest for configurations having the shortest O-O separation. The overlayer-oxygen–underlayer-oxygen distance and corresponding oxygen-oxygen force constant which yields a best fit to the experimental values are listed in Table I for all configurations. Some of the configurations require unrealistic force constants in order to obtain agreement with the 40-meV peak. For the overlayer oxygen in a *B* site and the underlayer oxygen in a t*B* site, the oxygen-oxygen distance is shorter than in molecular oxygen, yet weak O-O force constants increase the frequency of the low-energy peak significantly. For the overlayer oxygen at a *B* site and the underlayer at the o*C* site, the O-O distance is large, yet the O-O interaction must be assumed to be very large. If no interaction is assumed, the low-energy peak is at 47 instead of 40 meV. From these results it is clear that the overlayer oxygen must occupy the *C* sites of Fig. 2. This is the overlayer site also preferred by LEED[1]

TABLE I. Summary of overlayer-underlayer configurations and corresponding O-O distances and force constants which yield the best fit to experimentally determined mode frequencies. The force constant for molecular oxygen O_2 is 1180 N/m.

Oxygen location (overlayer-underlayer)	O-O distance (Å)	O-O force constant divided by O_2 force constant
B/t*B*	1.17	0
C/o*C*	1.75	1.025
C/mo*C*	1.94	1.953
C/t*B*	2.03	0.651
B/o*C*	2.41	6.508

and photoemission.[4]

There remain three possible underlayer sites: the t*B*, o*C*, and mo*C* sites. If no O-O interaction is assumed, the t*B* site gives a low-energy peak at 41 meV, and both o*C* and mo*C* sites give a peak at 47 meV. The agreement between calculated and measured frequencies is much less sensitive to the O-O force constant for t*B* underlayer sites than for o*C* and mo*C* underlayer sites. (See Table II.)

It is also instructive to examine the effects on mode energies when the overlayer is removed from these configurations. For the o*C* site, the low-energy peak experiences a large upward shift to 67 meV, and the 105-meV peak a small downward shift to 101 meV. For the t*B* site, the low-energy peak experiences a smaller upward shift to 55 meV, and the 105-meV peak remains virtually stationary. The experimental data in Fig. 1 show a measured low-energy peak shift from 40 to 50 meV after annealing, with little or no shift in the 105-meV peak. However, there is still some overlayer present after annealing and the full shift would not be measured. If one removes the underlayer, the overlayer peak for the t*B* site shifts from 80 to 73 meV, indicating that there may be up to 7-meV variation in the overlayer peak energy depending on the amount of adjacent underlayer oxygen. The additional width of the loss peaks could thus be attributed to nonuniformity in the distribution of O above and below the surface across the crystal face. From these results it appears that the underlayer oxygen must be in the t*B* site. This is the underlayer site predicted by Norman *et al.* based on SEXAFS.[2]

Eigenvectors obtained from the lattice-dynamical models provide a basis for qualitatively understanding

TABLE II. *z* components of the eigenvectors corresponding to each $\hat{z}$-polarized surface mode for the most likely configuration: overlayer O in the *C* site and underlayer oxygen in the t*B* site. Relative phase indicated by + or − sign.

Mode energy	40 meV	80 meV	105 meV
Layer			
O overlayer	+0.38	+0.37	+0.04
First layer Al	+0.11	−0.57	−0.12
O underlayer	−0.30	+0.02	+0.52
Second layer Al	−0.33	+0.20	−0.46

the relative peak intensities. Evans and Mills[10] have shown the EELS cross section for dipole scattering is given by

$$\frac{d\sigma(\omega_n,k_\parallel)}{d\Omega} \propto \frac{|\sum_l e_{nl}^* \xi_{nl}(k_\parallel)|^2}{\omega_n[1-\exp(\hbar\omega_n/k_BT)]} ,$$

where n labels the mode and the sum is over atomic layers l. For specular scattering $k_\parallel = 0$, and $\xi_{nl}(0)$ are the z components of the eigenvector of the particle in layer l in the nth mode. The theoretical evaluation of e_{nl}^*, the dynamic dipole "effective charge," requires a complicated quantum-mechanical calculation. For underlayer and overlayer oxygen in Al(111) it seems reasonable to assume that e^* is not strongly site dependent because the local chemical environment for the O sites is similar. Assuming $e_O^* = -e_{Al}^*$, the mode cross-section ratios can be estimated by summing over the two oxygen layers and the two surface Al layers. The lattice model shows that the two high-energy modes (80 and 105 meV) are produced by oxygen atoms vibrating 180° out of phase with neighboring Al atom planes. This corresponds to relatively large dynamic dipole moments. The low-energy mode is produced by overlayer-oxygen atoms vibrating in phase with the surface Al plane and the underlayer vibrating 180° out of phase with the surface Al plane. The relative amplitudes for this mode are smaller. The low-energy mode, although affected by the oxygen-oxygen interaction, is primarily due to coupling of the first- and second-layer Al planes through the underlayer oxygen. If the underlayer is allowed to interact with only the first or second Al layer, no low-energy mode appears.

This work was sponsored by the AFOSR under Grant No. AFOSR-80-0154, NSF under Grant No. DMR-8121916, and the Robert A. Welch Foundation.

[1]F. Soria, V. Martinez, M. C. Munoz, and J. L. Sacedon, Phys. Rev. B 24, 6926 (1981).
[2]D. Norman, S. Brennan, R. Jaeger, and J. Stohr, Surf. Sci. 105, L297 (1981).
[3]R. Michel, J. Gastaldi, C. Allasia, C. Jourdan, and J. Derrien, Surf. Sci. 95, 309 (1980).
[4]C. W. B. Martinson and S. A. Flodstrom, Solid State Commun. 30, 671 (1979).
[5]P. Hofmann, C. V. Muschwitz, K. Horn, K. Jacobi, A. M. Bradshaw, K. Kambe, and M. Scheffler, Surf. Sci. 89, 327 (1979).
[6]P. Hofmann, W. Wyrobisch, and A. M. Bradshaw, Surf. Sci. 80, 344 (1979).
[7]J. L. Erskine and R. L. Strong, Phys. Rev. B 25, 5547 (1982).
[8]G. P. Alldredge, R. E. Allen, and F. W. de Wette, Phys. Rev. B 4, 1648, 1661, 1682 (1971).
[9]L. Kleinman and D. M. Bylander (private communication) have performed first-principles calculations which indicate that the binding energy in the tetrahedral sites is not sufficiently large and that these sites also would cause larger shifts in the work function than those which are actually observed. They suggest that the actual position might be below the octahedral site, 0.6 Å above the second aluminum layer, with the surface aluminum layer relaxed inward by an amount which they have as yet not determined.
[10]E. Evans and D. L. Mills, Phys. Rev. B 5, 4126 (1972).